Published in final edited form as:
Cell Metab. 2010 May 5; 11(5): 353–363. doi:10.1016/j.cmet.2010.04.003.

Cardiac copper deficiency activates a systemic signaling mechanism that communicates with the copper acquisition and storage organs

Byung-Eun Kim[1], **Michelle L. Turski**[1], **Yasuhiro Nose**[1], **Michelle Casad**[2,3], **Howard A. Rockman**[2,3], and **Dennis J. Thiele**[1,*]

[1]Department of Pharmacology and Cancer Biology, Duke University Medical Center, Durham, North Carolina 27710

[2]Department of Medicine, Duke University Medical Center, Durham, North Carolina 27710

[3]Cell Biology, Duke University Medical Center, Durham, North Carolina 27710

Abstract

Copper (Cu) is an essential cofactor for a variety of metabolic functions and the regulation of systemic Cu metabolism is critical to human health. While dietary Cu is absorbed through the intestine, stored in the liver and mobilized into the circulation, systemic Cu homeostasis is poorly understood. We generated mice with a cardiac specific knock out of the Ctr1 Cu transporter, resulting in cardiac Cu deficiency (*Ctr1*$^{hrt/hrt}$) and severe cardiomyopathy. Unexpectedly, *Ctr1*$^{hrt/hrt}$ mice exhibited an increase in serum Cu levels and a concomitant decrease in hepatic Cu stores. Expression of the ATP7A Cu exporter, thought to function predominantly in intestinal Cu acquisition, was strongly increased in liver and intestine of *Ctr1*$^{hrt/hrt}$ mice. These studies identify ATP7A as a candidate for hepatic Cu mobilization in response to peripheral tissue demand and illuminate systemic regulation that signals the Cu status of the heart to Cu uptake and storage organs.

Introduction

Copper (Cu) is an essential element that has the ability to exist in two oxidation states, Cu^{+} and Cu^{2+}. This redox property of Cu has been harnessed during the evolution of Cu-containing enzymes, which use Cu as a cofactor during hydrolytic, electron transfer and oxygen-utilization reactions to carry out a diverse array of functions from mitochondrial oxidative phosphorylation to peptide hormone maturation (Kim et al., 2008; Madsen and Gitlin, 2007a). Consistent with the broad biochemical roles of Cu-dependent enzymes, Cu deficiency in mammals has been demonstrated to result in permanent impaired cognitive and motor function, embryonic and neonatal abnormalities and anemia (Madsen and Gitlin, 2007b; Prohaska, 2000). Although many of the proteins involved in Cu uptake and distribution at the cellular level have been identified, the mechanisms for the regulation of systemic Cu absorption in multi-cellular organisms is not well understood (Kim et al., 2008).

* correspondence should be addressed to D.J. Thiele (dennis.thiele@duke.edu).

Ctr1 is a homotrimeric integral membrane protein, conserved from yeast to humans, that transports Cu across the plasma membrane with high affinity and specificity (Hamza et al., 2003; Hua et al., 2009; Nose et al., 2006b). Intracellular Cu is routed to cytosolic Cu, Zn superoxide dismutase by the CCS Cu chaperone, to cytochrome oxidase through a series of mitochondrial-associated Cu binding proteins and to the secretory compartment by the Atox1 chaperone (Cobine et al., 2006; Culotta et al., 2006; Lutsenko et al., 2007). Atox1 delivers Cu to either of the structurally related ATP7A or ATP7B Cu transporting ATPases (Hamza et al., 2003; Linz and Lutsenko, 2007), through which Cu is pumped into the lumen of the secretory machinery for loading onto Cu-dependent proteins such as ferroxidases, lysyl oxidase and peptide hormone amidating enzymes (El Meskini et al., 2003; Hellman et al., 2002; Petris et al., 2000). In intestinal epithelial cells Cu is transported across the basolateral membrane by ATP7A, where it is transported via the portal circulation to the liver, the primary site of Cu storage. Excess liver Cu is removed by biliary excretion via the action of the ATP7B Cu pump and it has been proposed that an as yet unidentified Cu transporter may function in Cu mobilization from the liver to peripheral tissues (De Domenico et al., 2008; Lutsenko et al., 2008). While the coordinated actions of organs are likely to be critical for normal peripheral Cu homeostasis, and the hormonal regulation by hepcidin plays an important role in systemic iron metabolism (De Domenico et al., 2008; Roy et al., 2007), evidence for a regulatory mechanism by which hepatic Cu stores are mobilized to the peripheral circulation under conditions of Cu demand has not been reported.

Cardiac tissue exhibits a particularly high demand for Cu in order to sustain mitochondrial oxidative phosphorylation to generate large amount of energy for muscle contraction, peptide hormone biogenesis, oxidative stress protection and other critical functions (Medeiros et al., 1993). Animal models of dietary or genetically imposed Cu deficiency demonstrate severe cardiovascular dysfunction resulting in aneurysm, cardiac hypertrophy and other cardiovascular functional defects (Mandinov et al., 2003; Prohaska and Heller, 1982). Cardiac hypertrophy is an adaptive response to heart pressure overload due to pregnancy, exercise and other stresses, which enables the heart to increase its pumping activity via elevated contractility (Frey and Olson, 2003; Schannwell et al., 2002a). If the stressful stimuli persist, depending on the individual conditions such as genetic background and nutritional conditions, maladaptive hypertrophy becomes irreversible and frequently leads to cardiac dysfunction and heart failure (Carabello, 2002; Schannwell et al., 2002b). While Cu deficiency has been known to disrupt cardiovascular function and lead to cardiac hypertrophy, it has not been established whether Cu deficiency-induced cardiac hypertrophy is due to an overall peripheral Cu deficiency or an intrinsic cardiac-specific requirement for Cu to maintain normal function (Jiang et al., 2007; Kelly et al., 1974; Klevay, 2001; Pyatskowit and Prohaska, 2007).

Here we report the generation of a fruit fly and mouse model of Cu-deficiency mediated cardiac hypertrophy via cardiac-specific knock out of the Ctr1 Cu transporter. Our analysis of this mouse model demonstrates that a cardiac-specific Ctr1 knock out is sufficient to trigger a severe cardiac hypertrophy. While Cu accumulation in cardiac tissue from $Ctr1^{hrt/hrt}$ mice was decreased, we observed an unexpected increase in serum Cu levels and a concomitant decrease in hepatic Cu stores. Moreover, we observed a striking increase in the expression of the ATP7A Cu efflux pump in the liver and intestinal epithelial cells of $Ctr1^{hrt/hrt}$ mice, but not in other peripheral tissues or in wild type mice. These studies implicate ATP7A as a key component for hepatic Cu mobilization shortly after birth and during times of peripheral Cu deficiency. Moreover, these results uncover a systemic Cu homeostasis regulatory mechanism that signals the Cu status of the heart, and potentially other peripheral organs, to tissues involved in Cu uptake and storage.

Results

Dorsal vessel knockdown of *Drosophila* Ctr1A leads to cardiomyopathy

A dietary or genetically imposed peripheral Cu deficiency due to intestinal-specific ablation of Ctr1 results in severe dilated cardiomyopathy and cardiac hypertrophy (Nose et al., 2006a; Prohaska, 1983). To ascertain if Cu deficiency-induced cardiomyopathy is due to a cardiac-specific requirement for Cu, rather than a general Cu deficiency, we first generated a metazoan model with a cardiac-specific Ctr1 knockdown in fruit flies, as proof of principle. Previous studies established that the fruit fly, *Drosophila melanogaster*, is a facile experimental system for the identification of genes associated with adult human cardiomyopathy, as fly cardiovascular function can be evaluated by optical coherence tomography (Wolf et al., 2006). Moreover, flies heterozygous for the primary Cu transporter, Ctr1A, exhibit Cu remedial defects in heart beat rate and in the maturation of cardio-stimulatory peptides (Turski and Thiele, 2007). As shown in Figure 1A-D, RNAi-mediated knockdown of Ctr1A specifically in the dorsal vessel, the functional equivalent of the fly heart, resulted in increased end systolic dimensions along with reduced fractional shortening as compared to control flies. These studies suggest that metazoan cardiac-specific Cu deficiency is sufficient to generate a severe cardiomyopathy and prompted further investigation in a mammalian model system.

Generation of a cardiac specific Ctr1 knockout mouse model

To evaluate the consequences of a specific reduction in cardiac Cu load in mammals, mice were generated in which the gene encoding the Ctr1 Cu transporter was excised by crossing $Ctr1^{flox/flox}$ mice with mice specifically driving nuclear-localized Cre recombinase in cardiac tissue via the alpha-Myosin Heavy Chain (*MHC*) promoter (Agah et al., 1997). The cardiac-specific Ctr1 depleted mice, hereafter referred to as $Ctr1^{hrt/hrt}$, were born at the expected Mendelian frequency and exhibited normal growth for approximately 5 days as compared to wild type littermates. Within a week $Ctr1^{hrt/hrt}$ mice began to exhibit dramatic growth retardation, with the majority dying within three weeks after birth (Figures 2A-C). Immunoblotting of total protein extracts and diagnostic PCR analysis of DNA from several tissues revealed cardiac-specific and efficient knock-out of Ctr1 (Figures 2D and S1A, B, C). Accordingly, the steady state levels of the Cu chaperone for Cu, Zn superoxide dismutase, CCS and mitochondrial cytochrome oxidase subunit IV (COX IV), previously shown to be elevated or reduced, respectively, in response to Cu deficiency (Bertinato and L'Abbe, 2003; Caruano-Yzermans et al., 2006; Gybina and Prohaska, 2006; West and Prohaska, 2004), were altered as expected for a Cu-deficient heart (Figure 2D). Among several tissues analyzed, steady state levels of CCS were increased only in cardiac tissue from $Ctr1^{hrt/hrt}$ mice compared to control littermates (Figure S1C).

Cardiac-specific Ctr1 ablation is sufficient to trigger a severe cardiac hypertrophy

Despite $Ctr1^{hrt/hrt}$ mice being significantly smaller than age-matched control littermates (Figures 2A and 2B), hearts from $Ctr1^{hrt/hrt}$ mice were dramatically enlarged and the heart weight to total body weight ratio was increased nearly three-fold, suggesting that cardiac-specific loss of Ctr1 leads to cardiac hypertrophy (Figures 3A and 3B). To further investigate this anatomical phenotype, markers that are elevated with pathological cardiac hypertrophy were evaluated by RNA blotting (Dorn et al., 2003). As shown in Figure 3C, mRNA levels for atrial natriuretic peptide (ANP), b-type natriuretic peptide (BNP) and skeletal actin (SA) were dramatically elevated in both male and female $Ctr1^{hrt/hrt}$ mice as compared to control $Ctr1^{flox/flox}$ littermates. Immunohistochemical interrogation of fixed cardiac tissue from $Ctr1^{hrt/hrt}$ mice showed cardiomyocyte enlargement (Figure 3D), overt endocardial fibrosis (Figure 3E) and disordered sarcomere arrays, with enlarged cardiomyocytes harboring swollen mitochondria and morphologically irregular cristae observed by electron microscopy that are typical of a cardiac myopathic process (Figure 3F).

Physiological consequences of cardiac loss of Ctr1 in neonatal and adult mice

To investigate the physiological consequences of cardiac-specific Ctr1 knock out, heart function was evaluated by echocardiography and electrocardiography. *Ctr1*$^{hrt/hrt}$ mice of postnatal day 10 (P10) exhibited left ventricular dilation (both diastolic (LVDd) and systolic (LVDs)), increased left ventricular mass (LVm), decreased fractional shortening, and a marked decrease in heart rate (Figures 4A-C). Moreover, representative electrocardiagram recordings of P10 *Ctr1*$^{hrt/hrt}$ and *Ctr1*$^{flox/flox}$ littermates showed evidence for striking bradycardia and possibly heart block (Figure 4D). To further investigate the cardiac contractility of *Ctr1*$^{hrt/hrt}$ mice, we quantified the expression levels of a calcium pump, SERCA2 and its major regulator, phospholamban (PLB) (MacLennan and Kranias, 2003) in the heart of *Ctr1*$^{hrt/hrt}$ mice. While SERCA2 expression was marginally decreased, both PLB and phospho-PLB (Ser-16) exhibited dramatically elevated expression compared to control mice (Figure 4E), suggesting that cardiac calcium cycling is significantly disrupted in the *Ctr1*$^{hrt/hrt}$ mice.

These results from the constitutive cardiac-specific Ctr1 knock out suggest that Cu accumulation mediated by the Ctr1 Cu transporter is critical for the prevention of dilated cardiomyopathy during early postnatal stages. However, because the *MHC-Cre* transgene is expressed during embryonic development (Subramaniam et al., 1991) this could be due to a developmental requirement for cardiac Ctr1 in Cu uptake. To address this possibility a mouse line was generated with an inducible Cre transgene (*MHC-Cre-ER*) (Sohal et al., 2001; Xiong et al., 2007) in which cardiac-specific Cre recombinase was activated for Ctr1 excision only after administration of 4-OH-tamoxifen (OHT) to 2 or 7 month-old mice (Figure S2A). Consistent with a Cu-deficiency induced cardiomyopathy, both cohorts showed strong cardiac-specific reduction of Ctr1, an increase in the steady-state levels of the CCS Cu chaperone (Figure 4F) and decreased Cu levels (data not shown). These mice began to die at ~2 days after OHT administration (Figure S2B). Furthermore, these mice exhibited an enlarged heart (Figures S2C and S2D), dilated left ventricle with decreased fractional shortening, increased cardiac phospho-PLB expression (Figure S2D, E, F, G), and cardiomyocyte enlargement (Figure 4G) within 5 days after administration of OHT. Taken together, these results demonstrate that the Ctr1 Cu transporter is critical for maintenance of cardiac function and for the prevention of cardiomyopathy in both neonatal and adult mammals. Moreover, coupled with the results obtained from Ctr1A knock down experiments in the fly dorsal vessel, these results suggest a specific and evolutionarily conserved role for the Ctr1 Cu transporter in cardiovascular function.

A systemic copper signaling mechanism

Hearts from *Ctr1*$^{hrt/hrt}$ mice expressed significantly less Ctr1 in cardiac tissue and accumulated less Cu as compared to wild type littermates (Figure 5A). Hearts from *Ctr1*$^{hrt/hrt}$ mice also exhibited a strong diminution of mitochondrial cytochrome oxidase activity as compared to tissue from wild type litter-mates (Figure 5B), indicating that Ctr1 is the major Cu importer in the heart. Surprisingly while the Ctr1 gene is not excised and Ctr1 protein expression is not decreased in the liver of *Ctr1*$^{hrt/hrt}$ mice (Figures S1B and S1C), Cu levels in the liver are decreased by approximately 20% and serum Cu is elevated by approximately 30% (Figure 5A). No elevations in serum Fe or Zn were apparent in these same samples (Figures S3A and S3B). These observations suggested that under conditions of cardiac Cu deficiency, pools of Cu in the liver, the major storage organ, are reduced and there is a concomitant increase in Cu in the peripheral circulation. While the ATP7B Cu-transporting ATPase is known to efflux liver Cu into the bile for excretion, the mechanisms by which liver Cu storage pools are mobilized into the circulation are not known. We examined the expression levels of potential Cu exporting proteins in the liver and observed a dramatic elevation of the ATP7A Cu efflux pump in *Ctr1*$^{hrt/hrt}$ mice as compared to control littermates (Figure 5C). This was not anticipated, since ATP7A is not highly expressed in the liver in Cu adequate animals and a heptatic function for

ATP7A had not been previously identified. Semi-quantative RT-PCR revealed that ATP7A mRNA levels are strongly elevated in liver tissues from *Ctr1*$^{hrt/hrt}$ mice compared to control littermates (Figure 5D), whereas ATP7B steady state mRNA levels remained unchanged and ATP7B protein levels are rather marginally decreased (Figure 5F). Evaluation of ATP7A localization in the liver from *Ctr1*$^{hrt/hrt}$ mice revealed that while ATP7A is poorly expressed in wild type liver, in *Ctr1*$^{hrt/hrt}$ mice the ATP7A signal is strong and is enriched toward the sinusoidal space (Figure 5E). Moreover, liver and serum ceruloplasmin protein levels are unchanged in *Ctr1*$^{hrt/hrt}$ mice compare to control mice (Figure 5F and S3C). These results suggest that changes in liver and serum Cu levels in the *Ctr1*$^{hrt/hrt}$ mice are not due to differences in the synthesis or secretion of ATP7B or ceruloplasmin.

It is well established that the intestinal enterocyte is a key regulatory point for Cu absorption into the body (Llanos and Mercer, 2002; Nose et al., 2006a; Turnlund, 1998). However, little is known about how the small intestine responds to changes in the Cu status or Cu demands of peripheral tissues. Since expression of the ATP7A Cu transporting ATPase is strongly elevated in the liver of *Ctr1*$^{hrt/hrt}$ mice, we evaluated ATP7A in intestinal epithelial cells in this background. As shown in Figure 5G, ATP7A expression is dramatically elevated in the intestinal epithelial cells from *Ctr1*$^{hrt/hrt}$ mice as compared to control *Ctr1*$^{flox/flox}$ littermates. Moreover, these intestinal epithelial cells show a slight elevation of CCS, suggesting that these cells are somewhat Cu deficient. Levels of the intestinal glucose transporter, Glut-2 are unchanged in *Ctr1*$^{hrt/hrt}$ mice compare to control mice (Figure S3D). Elevated hepatic ATP7A levels were also observed from induced-cardiac Ctr1 deletion mice compare to control mice (Figure S3E). Taken together these results demonstrate that in response to cardiac-specific Cu deficiency, ATP7A Cu transporter levels are dramatically elevated in both the small intestine and liver, the primary sites of Cu absorption and storage, respectfully.

Hepatic ATP7A expression correlates with Cu mobilization

What physiological conditions would demand elevated ATP7A expression in the primary Cu uptake and Cu storage organs? Previous studies demonstrated that Cu levels in the liver of post-natal mice are high and that these levels gradually decrease as mice age under standard weaning and diet conditions (Allen et al., 2006; Pyatskowit and Prohaska, 2008). We tested whether decreased Cu status in the liver, as a function of time after birth, is associated with changes in the levels of ATP7A in mice reared on a normal diet. As shown in Figure 6A, expression levels of COX IV did not change significantly in the livers of mice over the first six months of life, suggesting that the liver maintained a level of Cu sufficient to sustain cytochrome oxidase assembly. The levels of liver ceruloplasmin, a Cu-dependent ferroxidase involved in Fe loading onto transferrin, are also not significantly altered in these mice. However, while liver ATP7A levels are very high immediately after birth, they strongly decrease in a time dependent manner such that ATP7A levels are only modestly detected 6 months after birth (Figure 6A). The hepatic Cu content in these mice demonstrated that decreased Cu levels are associated with decreased expression of hepatic ATP7A (Figure 6B). Notably, expression of ATP7A in the liver of P10 *Ctr1*$^{hrt/hrt}$ mice is strongly elevated beyond that of P10 wild type mice (Figure 6C) suggesting that the increased Cu demand in cardiac tissue of *Ctr1*$^{hrt/hrt}$ mice further enhances ATP7A expression. These data further suggest that ATP7A may function in hepatic Cu efflux early after birth, when Cu is being loaded into the periphery, and that this role diminishes after weaning as mice mature and reach an adequate Cu status.

Data presented here demonstrate that a genetically programmed cardiac Cu deficiency results in dramatically elevated intestinal epithelial and hepatic ATP7A expression and a parallel decrease in liver Cu stores and increase in circulating Cu. These observations are consistent with ATP7A playing an unanticipated role in the mobilization of hepatic Cu stores. To test

whether ATP7A could play such a role under more physiologically relevant conditions, we examined ATP7A protein levels from wild type pups reared on a Cu deficient (D) diet or a Cu adequate (A) diet for 5 weeks beginning post natal day two. As shown in Figure 6D, ATP7A levels in intestinal epithelial cells (IEC) from mice reared on a Cu deficient diet are dramatically elevated as compared to mice reared on a normal diet. The steady state CCS levels were elevated and COX IV levels decreased in tissues from mice raised on a Cu deficient diet, with the changes of COX IV and CCS particularly evident in the heart and consistent with higher Cu demands for cardiac function. Limited Cu availability from diet as well as the efflux of Cu via the action of ATP7A in intestinal epithelial cells may cause a Cu deficiency in the cells resulting in higher level of CCS. Interestingly, the dietary Cu deficiency regimen used here did not result in increased hepatic ATP7A. While the reason why ATP7A in the liver was not increased in these mice is not clear, it is possible that the stored Cu in the liver has already been depleted after this period of growth on a Cu-deficient diet. Taken together, these data strongly suggest that ATP7A plays an important role in the mobilization of hepatic Cu stores and further, that elevating intestinal Cu absorption may be a primary mode of enhancing Cu supplies to peripheral tissues after a stage when liver Cu stores have been diminished.

ATP7A activation by a circulating signal from *Ctr1*$^{hrt/hrt}$ mice

To further test if the *Ctr1*$^{hrt/hrt}$ mice possess a circulating signal that induces ATP7A expression, human primary umbilical vein endothelial cells (HUVEC) were treated with serum from control or *Ctr1*$^{hrt/hrt}$ mice. The data shown in Figure 7A demonstrate that treatment of HUVEC cells with serum from *Ctr1*$^{hrt/hrt}$ mice increased ATP7A expression beyond that of serum from control mice. Increased CCS levels in the cells treated with serum from *Ctr1*$^{hrt/hrt}$ mice suggest decreased intracellular Cu levels due to the action of ATP7A pumping Cu from these cells. Furthermore, treatment of a human intestinal epithelial-like cell line (Caco-2) with serum from *Ctr1*$^{hrt/hrt}$ mice also increased ATP7A expression compared to serum from control mice (Figure 7B). These data suggest that *Ctr1*$^{hrt/hrt}$ mice possess a positively acting diffusible signal that is able to stimulate expression of the ATP7A Cu efflux pump.

Discussion

The experimental results presented here demonstrate that cardiac-specific loss of the Ctr1 Cu transporter results in a reduction in cardiac Cu levels and the generation of morphological, histological, molecular and physiological hallmarks of cardiac hypertrophy. These observations underscore the strong cardiac-intrinsic requirement for Cu acquisition, driven by the evolutionary conserved Ctr1 Cu transporter, rather than a more global peripheral Cu deficiency that impacts on cardiac function. While cardiac tissue has a high demand for Cu to support oxidative phosphorylation, oxidative stress protection and other functions, it is currently not well understood which cardiac functions are exquisitely sensitive to Cu deficiency to manifest in a cardiomyopathy, both in fruit flies and in mice. Mutations in the human SCO2 gene, encoding a protein involved in the delivery of Cu to mitochondrial cytochrome oxidase, have been shown to cause fatal infantile cardiomyopathy (Jaksch et al., 2000) and ATP7A plays an important role in the regulation of extracellular superoxide dismutase (EC-SOD) activity and vascular nitric oxide signaling (Qin et al., 2008), further underscoring the severe cardiac health consequences of both dietary and genetically imposed defects in Cu acquisition or cellular Cu delivery.

One mediator of cardiac hypertrophy, the NFAT phosphatase calcineurin, might have a link to Cu-metabolism via functional interactions with Cu, Zn SOD (Wang et al., 1996). However, given that mice lacking Cu, Zn SOD do not develop apparent cardiac hypertrophy (Elchuri et al., 2005; Yoshida et al., 2000), it is unlikely that Cu, Zn SOD is the critical Cu deficiency-

sensitive target that leads to hypertrophy. A recent study in mice suggested Cu supplementation partially prevents hypertrophic cardiac dysfunction through the copper chaperone for Cu, Zn SOD (CCS) mediated HIF-1alpha activation and VEGF expression (Jiang et al., 2007). However, no causal relationship between CCS and cardiac hypertrophy has been established and neither CCS nor SOD1 knock out mice have been reported to suffer from cardiac hypertrophy. The cardiac-specific Ctr1 knock out mice will be a valuable animal model for deciphering the mechanisms by which Cu deficiency induces cardiac hypertrophy.

The components involved in the acquisition, distribution and utilization of Cu at the cellular level, and their modes of action, have been extensively investigated. However, the precise mechanisms by which Cu is transfered from intestinal epithelial cells to the portal circulation and is then mobilized from hepatic stores to the periphery are poorly understood. Furthermore, while it is well established that the intestinal enterocyte is key regulatory point for Cu absorption into the body, how these cells respond to changes in Cu status in the periphery remains poorly understood. Studies on cardiac-specific Ctr1 knock out mice presented here suggest that ATP7A may be responsible for Cu mobilization from the liver when peripheral tissues become Cu-deficient. This possibility was unexpected, since ATP7A is thought to function primarily in extra-hepatic tissues and its expression levels in the liver of mature mice are very low (Paynter et al., 1994). However, given the localization of ATP7A in endothelial cells lining hepatic sinusoidal spaces, and the dramatic elevation of hepatic ATP7A mRNA and protein levels in $Ctr1^{hrt/hrt}$ mice, these observations are consistent with a role for ATP7A in the mobilization of hepatic Cu stores when one or more tissues in the periphery are Cu deficient. Moreover, given the high level expression of ATP7A in early post-natal mice, when liver Cu stores are high and gradually diminish over time to maturity, the ATP7A protein expression data are also consistent with a role for ATP7A in hepatic Cu mobilization during postnatal development.

An unexpected observation from the analysis of $Ctr1^{hrt/hrt}$ mice is the diminution of liver Cu stores in parallel with increases in serum Cu. These changes, in concert with the dramatically increased levels of ATP7A in both intestinal epithelial cells and in the liver, suggest that the Cu deficient cardiac tissue from $Ctr1^{hrt/hrt}$ mice may be able to communicate with the intestine and the liver to enhance the expression of the ATP7A Cu exporter from the sites of dietary uptake and storage. Since $Ctr1^{hrt/hrt}$ mice do not have elevated serum Zn or Fe levels compared to wild type littermates, this would be consistent with a signal from the heart that reports on the cardiac Cu status specifically, rather than metals in general. Interestingly, analysis of wild type mice reared on a Cu-limited diet revealed that ATP7A expression was dramatically elevated only in intestinal epithelial cells. While this may reflect differences in peripheral Cu deficiency or timing between the $Ctr1^{hrt/hrt}$ mice and dietary Cu deficiency of wild type mice, it may also suggest that intestinal Cu uptake is the major target tissue for regulation after hepatic Cu stores are strongly depleted in adult mice.

These results suggest the existence a diffusible systemic Cu regulatory system that is reminiscent of the hepcidin-mediated control of systemic iron homeostasis. In response to Fe overload, the liver produces elevated levels of mRNA encoding hepcidin, a polypeptide that interacts with the ferroportin Fe exporter on the basolateral membrane of intestinal epithelial cells to shut down Fe efflux into the circulation (De Domenico et al., 2008; Muckenthaler, 2008; Nemeth et al., 2004).

Our study suggests that the Cu-deficient heart alters the function or expression of a molecule that, directly or indirectly, positively influences ATP7A expression in the liver and intestine. Recent studies in tissue-culture models suggest that ATP7A and ATP7B are regulated by lactational hormones, inflammatory cytokines, lipopolysaccharide and growth factors (Ackland et al., 1999; Hardman et al., 2007; Michalczyk et al., 2008; White et al., 2009),

demonstrating the potential for small molecule regulation of systemic Cu metabolism. More extensive studies will be needed to comprehensively test this possibility and to understand the precise signals and regulatory events that lead to increases in ATP7A expression as a mechanism to enhance Cu acquisition and mobilization during fluctuations in Cu availability.

Experimental Procedures

Generation of cardiac specific Ctr1 conditional knock out mice

Ctr1-floxed (*Ctr1*$^{flox/flox}$) mice have been described (Nose et al., 2006a). *Ctr1*$^{flox/flox}$ mice were crossbred with *alpha-MHC-Cre* mice (Center for Cardiovascular Development, Baylor College of Medicine) to generate *MHC-Cre; Ctr1*$^{flox/+}$ mice. *The MHC-Cre; Ctr1*$^{flox/+}$ mice were crossbred with *Ctr1*$^{flox/flox}$ mice, and *Ctr*$^{hrt/hrt}$ mice were obtained. The genotypes of offspring from the cross as well as tissue excision of Ctr1 were determined by standard PCR method as described (Nose et al., 2006a). Age matched siblings were used for all experiments. To generate inducible cardiac-specific Ctr1 knock out mice *Ctr1*$^{flox/flox}$ mice were crossbred with *alpha-MHC-Cre-ER* mice (Jackson Laboratory) to generate *MHC-Cre-ER; Ctr1*$^{flox/+}$ mice. The *MHC-Cre-ER; Ctr1*$^{flox/+}$ mice were crossbred with *Ctr1*$^{flox/flox}$ mice, and *MHC-Cre-ER; Ctr1*$^{flox/flox}$ mice were obtained. 4-hyroxytamoxifen (4-OHT) was prepared as described previously (Indra et al., 1999). Two month or seven month-old *Ctr1*$^{flox/flox}$ mice and *MHC-Cre-ER; Ctr1*$^{flox/flox}$ mice were injected intraperitoneally with 100 μl of a 4-OHT stock solution (10mg/ml) for 5 consecutive days and sacrificed either after the last injection or 3 to 5 days after the final injection. All animal protocols were approved by the Duke University Institutional Animal Care & Use Committee.

Tissue preparation and analysis

Tissues were dissected after perfusion with phosphate-buffered saline (pH 7.4; PBS), frozen in liquid nitrogen, and stored at -80°C until use. Dissected tissues were homogenized in ice-cold cell lysis buffer (PBS pH7.4, 1% triton X-100, 0.1% sodium dodecyl sulfate (SDS), 1mM EDTA) containing protease inhibitor cocktail (Roche). Homogenates were incubated on ice for 30 min and centrifuged at 16,000×g for 10 min at 4 °C. The supernatants were used for immunoblotting. Equal amounts of protein (100 μg/lane) were fractionated on a 4-20 % gradient gel (BioRad). Anit-Ctr1 antibody (Nose et al., 2006a), anti-CCS antibody (Santa Cruz) and anti-SOD1 (BD bioscience) were used at a 1:2,000 dilution. Anti-Tubulin (Sigma) antibody and anti-COX IV antibody (Invitrogen) were used at 1:5,000 dilution and 1:4,000 dilution, respectively. Anti-SERCA2 antibody (Santa Cruz) was used at a 1:1,000 dilution. Anti-phospholamban antibody (Santa Cruz) and anti-phospho-phospholamban (Upstate) were used according to the provider's instructions. Phosphatase inhibitor cocktail (Thermo Scientific) was included in the lysis buffer and gels were run in duplicate for P-PLB westerns. Copper concentrations were measured from nitric acid-digested tissues by inductively coupled plasma mass spectrometry (ICP-MS) as described (Nose et al., 2006a). The values were normalized to tissue wet weight. For cytochrome oxidase assays, tissues were homogenized in 5 to 10 volumes of 50 mM phosphate buffer (pH 6.8) containing 0.5% Tween 80 and incubated on ice for 10 min. Protein concentrations were measured by the BioRad Protein DC Assay kit (BioRad) and cytochrome oxidase activity was measured using a Cytochrome C Oxidase Assay Kit (Sigma).

Histology

For hematoxylin and eosin (H&E) staining and immunohistochemistry, mice were euthanized and perfused with PBS (pH 7.4). Tissues were then dissected and fixed in 4% paraformaldehyde at 4°C overnight with gentle agitation. After fixation, tissues were dehydrated in 70% ethanol and embedded in paraffin. Six micrometer-thick sections were either stained with hematoxylin and eosin or used for immunohistochemistry. After deparaffinization and hydrolysis in PBS,

immunohistochemical staining was performed with the Super Sensitive Link-Labeled IHC Detection System (BioGenex, San Ramon, CA). Ten percent normal goat serum (Sigma, Saint Louis, MO) in PBS was used for blocking. Anti-ATP7A (1:200 dilution in 1% normal goat serum-PBS) was used as primary antibody for 1 hr at room temperature. After developing using DAB substrate, sections were counter-stained with hematoxylin. For electron microscopy, heart tissue was immersed in a fixative containing 2% glutaraldehyde immediately after dissection and incubated at 4°C overnight. Sectioning, staining, microscopy and image capture were carried out via the histology service core of the Department of Pathology, Duke University Medical Center (Durham, NC).

RNA analysis

Total RNA was isolated from mouse heart using the RNeasy Kit (Qiagen). RNA blotting was performed by standard methods using 20μg total RNA from cardiac tissue. Membranes were probed with ^{32}P-labeled DNA derived from ANF, BNP and SA cDNA sequences. For semi quantitative RT-PCR, cDNA was synthesized with SuperScript™ III Kit (Invitrogen) and the target genes were amplified using primers listed in Supplementary Table, electrophoresed on a 2% agarose gel, and visualized by ethidium bromide staining.

Echocardiography and Electrocardiography

Cardiac function and left ventricle dimensions were evaluated by Echocardiography in conscious mice as previously described (Esposito et al., 2000). Electrocardiography was performed under light anesthetizia (isofluorane inhalation).

Dietary experiments

Dams from wild type mice were fed Cu-adequate or Cu-deficient diets (Teklad Laboratories, Madison, WI) beginning on the 2nd day post delivery with their pups. The Cu deficient diet has been previously described (Kuo et al., 2006). The mice were weaned at 3 weeks of age. After weaning, mice were maintained on the same normal or Cu deficient diet for 2 weeks.

Supplementary Material

Refer to Web version on PubMed Central for supplementary material.

Acknowledgments

The authors gratefully acknowledge critical comments on the manuscript from Nancy Andrews, Karin Finberg, Tomasa Barrientos and members of the Thiele laboratory and the technical assistance of Scott McNaughton. ATP7A antibody was a generous gift from Michael Petris and Betty Eipper and ATP7B antibody from Jonathan Gitlin. This work was supported by NIH grants DK074192 and ES010356 to D.J.T and HL-56687 and HL-083065 to H.A.R. and a grant from the International Copper Association, Ltd. to D.J.T. M.L.T was a trainee of the Duke University Program in Genetics and Genomics. B.-E. K. was supported in part by a Leon Golberg Memorial Postdoctoral Fellowship and American Heart Association Postdoctoral Fellowship (09POST2251047).

References

Ackland ML, Anikijenko P, Michalczyk A, Mercer JFB. Expression of the Menkes copper-transporting ATPases, MNK, in the lactating human breast: possible role in copper transport into milk. J Histochem Cytochem 1999;47:1553–1562. [PubMed: 10567439]

Agah R, Frenkel PA, French BA, Michael LH, Overbeek PA, Schneider MD. Gene recombination in postmitotic cells. Targeted expression of Cre recombinase provokes cardiac-restricted, site-specific rearrangement in adult ventricular muscle in vivo. J Clin Invest 1997;100:169–179. [PubMed: 9202069]

Allen KJ, Buck NE, Cheah DM, Gazeas S, Bhathal P, Mercer JF. Chronological changes in tissue copper, zinc and iron in the toxic milk mouse and effects of copper loading. Biometals 2006;19:555–564. [PubMed: 16937262]

Bertinato J, L'Abbe MR. Copper modulates the degradation of copper chaperone for Cu,Zn superoxide dismutase by the 26 S proteosome. J Biol Chem 2003;278:35071–35078. [PubMed: 12832419]

Carabello BA. Concentric versus eccentric remodeling. J Card Fail 2002;8:S258–263. [PubMed: 12555129]

Caruano-Yzermans AL, Bartnikas TB, Gitlin JD. Mechanisms of the copper-dependent turnover of the copper chaperone for superoxide dismutase. J Biol Chem 2006;281:13581–13587. [PubMed: 16531609]

Cobine PA, Pierrel F, Winge DR. Copper trafficking to the mitochondrion and assembly of copper metalloenzymes. Biochim Biophys Acta 2006;1763:759–772. [PubMed: 16631971]

Culotta VC, Yang M, O'Halloran TV. Activation of superoxide dismutases: putting the metal to the pedal. Biochim Biophys Acta 2006;1763:747–758. [PubMed: 16828895]

De Domenico I, McVey Ward D, Kaplan J. Regulation of iron acquisition and storage: consequences for iron-linked disorders. Nat Rev Mol Cell Biol 2008;9:72–81. [PubMed: 17987043]

Dorn GW 2nd, Robbins J, Sugden PH. Phenotyping hypertrophy: eschew obfuscation. Circ Res 2003;92:1171–1175. [PubMed: 12805233]

El Meskini R, Culotta VC, Mains RE, Eipper BA. Supplying copper to the cuproenzyme peptidylglycine alpha-amidating monooxygenase. J Biol Chem 2003;278:12278–12284. [PubMed: 12529325]

Elchuri S, Oberley TD, Qi W, Eisenstein RS, Jackson Roberts L, Van Remmen H, Epstein CJ, Huang TT. CuZnSOD deficiency leads to persistent and widespread oxidative damage and hepatocarcinogenesis later in life. Oncogene 2005;24:367–380. [PubMed: 15531919]

Esposito G, Santana LF, Dilly K, Cruz JD, Mao L, Lederer WJ, Rockman HA. Cellular and functional defects in a mouse model of heart failure. Am J Physiol Heart Circ Physiol 2000;279:H3101–3112. [PubMed: 11087268]

Frey N, Olson EN. Cardiac hypertrophy: the good, the bad, and the ugly. Annu Rev Physiol 2003;65:45–79. [PubMed: 12524460]

Gybina AA, Prohaska JR. Variable response of selected cuproproteins in rat choroid plexus and cerebellum following perinatal copper deficiency. Genes Nutr 2006;1:51–59. [PubMed: 18850220]

Hamza I, Prohaska J, Gitlin JD. Essential role for Atox1 in the copper-mediated intracellular trafficking of the Menkes ATPase. Proc Natl Acad Sci U S A 2003;100:1215–1220. [PubMed: 12538877]

Hardman B, Michalczyk A, Greenough M, Camakaris J, Mercer JF, Ackland ML. Hormonal regulation of the Menkes and Wilson copper-transporting ATPases in human placental Jeg-3 cells. Biochem J 2007;402:241–250. [PubMed: 17109627]

Hellman NE, Kono S, Mancini GM, Hoogeboom AJ, De Jong GJ, Gitlin JD. Mechanisms of copper incorporation into human ceruloplasmin. J Biol Chem 2002;277:46632–46638. [PubMed: 12351628]

Hua H, Georgiev O, Schaffner W, Steiger D. Human copper transporter Ctr1 is functional in Drosophila, revealing a high degree of conservation between mammals and insects. J Biol Inorg Chem. 2009

Indra AK, Warot X, Brocard J, Bornert JM, Xiao JH, Chambon P, Metzger D. Temporally-controlled site-specific mutagenesis in the basal layer of the epidermis: comparison of the recombinase activity of the tamoxifen-inducible Cre-ER(T) and Cre-ER(T2) recombinases. Nucleic Acids Res 1999;27:4324–4327. [PubMed: 10536138]

Jaksch M, Ogilvie I, Yao J, Kortenhaus G, Bresser HG, Gerbitz KD, Shoubridge EA. Mutations in SCO2 are associated with a distinct form of hypertrophic cardiomyopathy and cytochrome c oxidase deficiency. Hum Mol Genet 2000;9:795–801. [PubMed: 10749987]

Jiang Y, Reynolds C, Xiao C, Feng W, Zhou Z, Rodriguez W, Tyagi SC, Eaton JW, Saari JT, Kang YJ. Dietary copper supplementation reverses hypertrophic cardiomyopathy induced by chronic pressure overload in mice. J Exp Med 2007;204:657–666. [PubMed: 17339407]

Kelly WA, Kesterson JW, Carlton WW. Myocardial lesions in the offspring of female rats fed a copper deficient diet. Exp Mol Pathol 1974;20:40–56. [PubMed: 4361723]

Kim BE, Nevitt T, Thiele DJ. Mechanisms for copper acquisition, distribution and regulation. Nat Chem Biol 2008;4:176–185. [PubMed: 18277979]

Klevay LM. Iron overload can induce mild copper deficiency. J Trace Elem Med Biol 2001;14:237–240. [PubMed: 11396784]

Kuo YM, Gybina AA, Pyatskowit JW, Gitschier J, Prohaska JR. Copper transport protein (Ctr1) levels in mice are tissue specific and dependent on copper status. J Nutr 2006;136:21–26. [PubMed: 16365053]

Linz R, Lutsenko S. Copper-transporting ATPases ATP7A and ATP7B: cousins, not twins. J Bioenerg Biomembr 2007;39:403–407. [PubMed: 18000748]

Llanos RM, Mercer JF. The molecular basis of copper homeostasis copper-related disorders. DNA Cell Biol 2002;21:259–270. [PubMed: 12042066]

Lutsenko S, Gupta A, Burkhead JL, Zuzel V. Cellular multitasking: the dual role of human Cu-ATPases in cofactor delivery and intracellular copper balance. Arch Biochem Biophys 2008;476:22–32. [PubMed: 18534184]

Lutsenko S, LeShane ES, Shinde U. Biochemical basis of regulation of human copper-transporting ATPases. Arch Biochem Biophys 2007;463:134–148. [PubMed: 17562324]

MacLennan DH, Kranias EG. Phospholamban: a crucial regulator of cardiac contractility. Nat Rev Mol Cell Biol 2003;4:566–577. [PubMed: 12838339]

Madsen E, Gitlin JD. Copper and iron disorders of the brain. Annu Rev Neurosci 2007a;30:317–337. [PubMed: 17367269]

Madsen E, Gitlin JD. Copper deficiency. Curr Opin Gastroenterol 2007b;23:187–192. [PubMed: 17268249]

Mandinov L, Mandinova A, Kyurkchiev S, Kyurkchiev D, Kehayov I, Kolev V, Soldi R, Bagala C, de Muinck ED, Lindner V, et al. Copper chelation represses the vascular response to injury. Proc Natl Acad Sci U S A 2003;100:6700–6705. [PubMed: 12754378]

Medeiros DM, Davidson J, Jenkins JE. A unified perspective on copper deficiency and cardiomyopathy. Proc Soc Exp Biol Med 1993;203:262–273. [PubMed: 8516340]

Michalczyk A, Bastow E, Greenough M, Camakaris J, Freestone D, Taylor P, Linder M, Mercer J, Ackland ML. ATP7B expression in human breast epithelial cells is mediated by lactational hormones. J Histochem Cytochem 2008;56:389–399. [PubMed: 18180385]

Muckenthaler MU. Fine tuning of hepcidin expression by positive and negative regulators. Cell Metab 2008;8:1–3. [PubMed: 18590684]

Nemeth E, Tuttle MS, Powelson J, Vaughn MB, Donovan A, Ward DM, Ganz T, Kaplan J. Hepcidin regulates cellular iron efflux by binding to ferroportin and inducing its internalization. Science 2004;306:2090–2093. [PubMed: 15514116]

Nose Y, Kim BE, Thiele DJ. Ctr1 drives intestinal copper absorption and is essential for growth, iron metabolism, and neonatal cardiac function. Cell Metab 2006a;4:235–244. [PubMed: 16950140]

Nose Y, Rees EM, Thiele DJ. Structure of the Ctr1 copper trans'PORE'ter reveals novel architecture. Trends Biochem Sci 2006b;31:604–607. [PubMed: 16982196]

Paynter JA, Grimes A, Lockhart P, Mercer JFB. Expression of the Menkes gene homologue in mouse tissues: lack of effect of copper on the mRNA levels. FEBS lett 1994;351:186–190. [PubMed: 8082762]

Petris MJ, Strausak D, Mercer JF. The Menkes copper transporter is required for the activation of tyrosinase. Hum Mol Genet 2000;9:2845–2851. [PubMed: 11092760]

Prohaska JR. Changes in tissue growth, concentrations of copper, iron, cytochrome oxidase and superoxide dismutase subsequent to dietary or genetic copper deficiency in mice. J Nutr 1983;113:2048–2058. [PubMed: 6312000]

Prohaska JR. Long-term functional consequences of malnutrition during brain development: copper. Nutrition 2000;16:502–504. [PubMed: 10906536]

Prohaska JR, Heller LJ. Mechanical properties of the copper-deficient rat heart. J Nutr 1982;112:2142–2150. [PubMed: 6215471]

Pyatskowit JW, Prohaska JR. Rodent brain and heart catecholamine levels are altered by different models of copper deficiency. Comp Biochem Physiol C Toxicol Pharmacol 2007;145:275–281. [PubMed: 17287146]

Pyatskowit JW, Prohaska JR. Copper deficient rats and mice both develop anemia but only rats have lower plasma and brain iron levels. Comp Biochem Physiol C Toxicol Pharmacol 2008;147:316–323. [PubMed: 18178529]

Qin Z, Gongora MC, Ozumi K, Itoh S, Akram K, Ushio-Fukai M, Harrison DG, Fukai T. Role of Menkes ATPase in angiotensin II-induced hypertension: a key modulator for extracellular superoxide dismutase function. Hypertension 2008;52:945–951. [PubMed: 18768397]

Roy CN, Mak HH, Akpan I, Losyev G, Zurakowski D, Andrews NC. Hepcidin antimicrobial peptide transgenic mice exhibit features of the anemia of inflammation. Blood 2007;109:4038–4044. [PubMed: 17218383]

Schannwell CM, Schneppenheim M, Plehn G, Marx R, Strauer BE. Left ventricular diastolic function in physiologic and pathologic hypertrophy. Am J Hypertens 2002a;15:513–517. [PubMed: 12074352]

Schannwell CM, Zimmermann T, Schneppenheim M, Plehn G, Marx R, Strauer BE. Left ventricular hypertrophy and diastolic dysfunction in healthy pregnant women. Cardiology 2002b;97:73–78. [PubMed: 11978952]

Sohal DS, Nghiem M, Crackower MA, Witt SA, Kimball TR, Tymitz KM, Penninger JM, Molkentin JD. Temporally regulated and tissue-specific gene manipulations in the adult and embryonic heart using a tamoxifen-inducible Cre protein. Circ Res 2001;89:20–25. [PubMed: 11440973]

Subramaniam A, Jones WK, Gulick J, Wert S, Neumann J, Robbins J. Tissue-specific regulation of the alpha-myosin heavy chain gene promoter in transgenic mice. J Biol Chem 1991;266:24613–24620. [PubMed: 1722208]

Turnlund JR. Human whole-body copper metabolism. Am J Clin Nutr 1998;67:960S–964S. [PubMed: 9587136]

Turski ML, Thiele DJ. Drosophila Ctr1A functions as a copper transporter essential for development. J Biol Chem 2007;282:24017–24026. [PubMed: 17573340]

Wang X, Culotta VC, Klee CB. Superoxide dismutase protects calcineurin from inactivation. Nature 1996;383:434–437. [PubMed: 8837775]

West EC, Prohaska JR. Cu,Zn-superoxide dismutase is lower and copper chaperone CCS is higher in erythrocytes of copper-deficient rats and mice. Exp Biol Med (Maywood) 2004;229:756–764. [PubMed: 15337829]

White C, Lee J, Kambe T, Fritsche K, Petris MJ. A role for the ATP7A copper-transporting ATPase in macrophage bactericidal activity. J Biol Chem. 2009

Wolf MJ, Amrein H, Izatt JA, Choma MA, Reedy MC, Rockman HA. Drosophila as a model for the identification of genes causing adult human heart disease. Proc Natl Acad Sci U S A 2006;103:1394–1399. [PubMed: 16432241]

Xiong D, Yajima T, Lim BK, Stenbit A, Dublin A, Dalton ND, Summers-Torres D, Molkentin JD, Duplain H, Wessely R, et al. Inducible cardiac-restricted expression of enteroviral protease 2A is sufficient to induce dilated cardiomyopathy. Circulation 2007;115:94–102. [PubMed: 17190866]

Yoshida T, Maulik N, Engelman RM, Ho YS, Das DK. Targeted disruption of the mouse Sod I gene makes the hearts vulnerable to ischemic reperfusion injury. Circ Res 2000;86:264–269. [PubMed: 10679476]

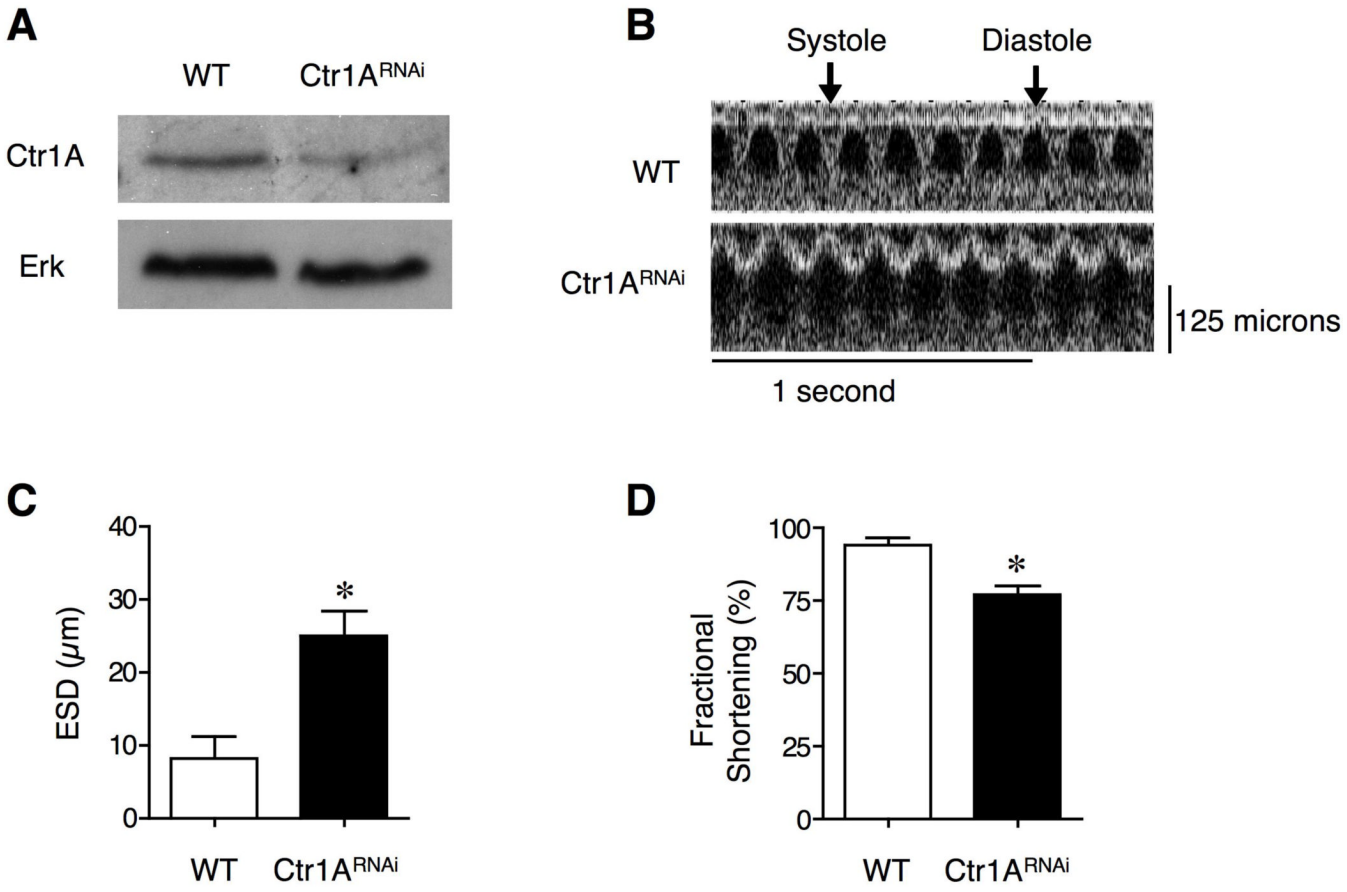

Figure 1. Cardiac-specific knockdown of the *Drosophila* Ctr1A Cu ion channel

(**A**) Knock down of Ctr1A in the dorsal vessel. Immunoblot of crudely dissected *Drosophila* dorsal vessel from wild type (WT) and TinCGal4/UAS-Ctr1A^{RNAi} flies (Ctr1^{RNAi}). Total tissue protein extracts were probed with anti-Ctr1A peptide antibody or anti-ERK as a loading control. (**B**) Representative optical coherence tomography (OCT) images for wild type and TinCGal4/UAS-Ctr1A^{RNAi} flies. (**C**) End systolic dimension (ESD) measurements for wild type and TinCGal4/UAS-Ctr1A^{RNAi} flies. Error bars, s.d., *P = 0.00073 versus wild type. (**D**) Fractional shortening measurements for wild type and TinCGal4/UAS-Ctr1A^{RNAi} flies. Error bars, s.d., *P < 0.001 versus wild type.

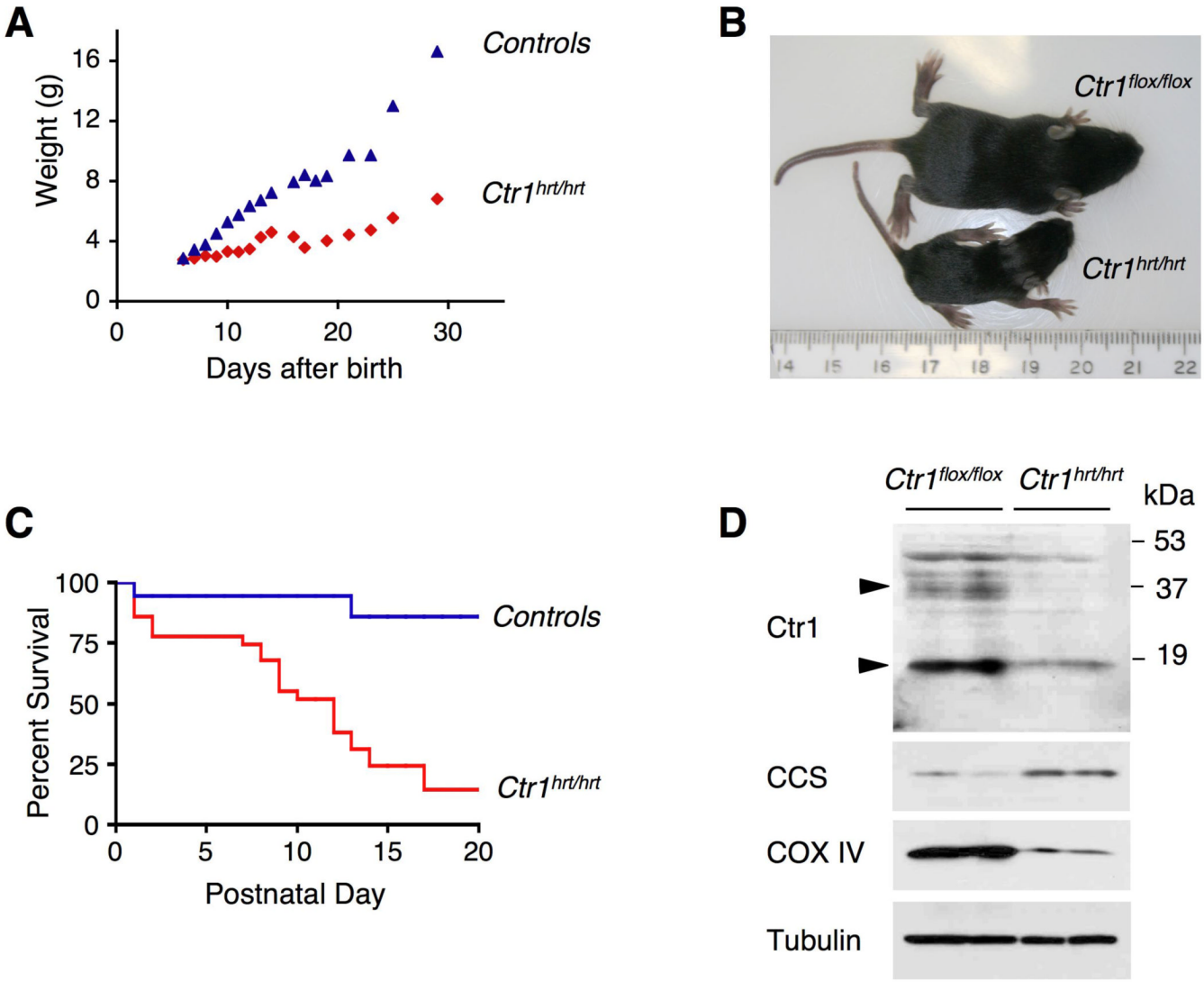

Figure 2. Generation of a cardiac-specific knock-out of the mouse Ctr1 gene

(**A**) Growth of *Ctr1*$^{hrt/hrt}$ mice. The body mass in grams (g) for *Ctr1*$^{hrt/hrt}$ mice (red) or control littermates (blue) as a function of age after birth in days is shown. (**B**) *Ctr1*$^{hrt/hrt}$ and *Ctr1*$^{flox/flox}$ littermates at P10. A ruler is included as a size reference (in cm). (**C**) Kaplan-Meier plot showing postnatal survival of control (blue, n=69; *Ctr1*$^{flox/flox}$, *Ctr1*$^{flox/+}$ and *Ctr*$^{hrt/+}$) and *Ctr1*$^{hrt/hrt}$ mice (red, n=25). (**D**) SDS-PAGE analysis of total Triton X-100 solubilized heart extracts of two representative *Ctr1*$^{flox/flox}$ and *Ctr1*$^{hrt/hrt}$ mice. Tissues were probed for Ctr1, CCS (copper chaperone for Cu, Zn superoxide dismutase), COX IV (mitochondrial cytochrome oxidase subunit V) and Tubulin as a loading control. The arrows indicate the positions of monomeric (at approximately 17kD) and heterogeneous glycosylated form (at approximately 35 kD) of Ctr1, both of which are dramatically reduced in the *Ctr1*$^{hrt/hrt}$ mice.

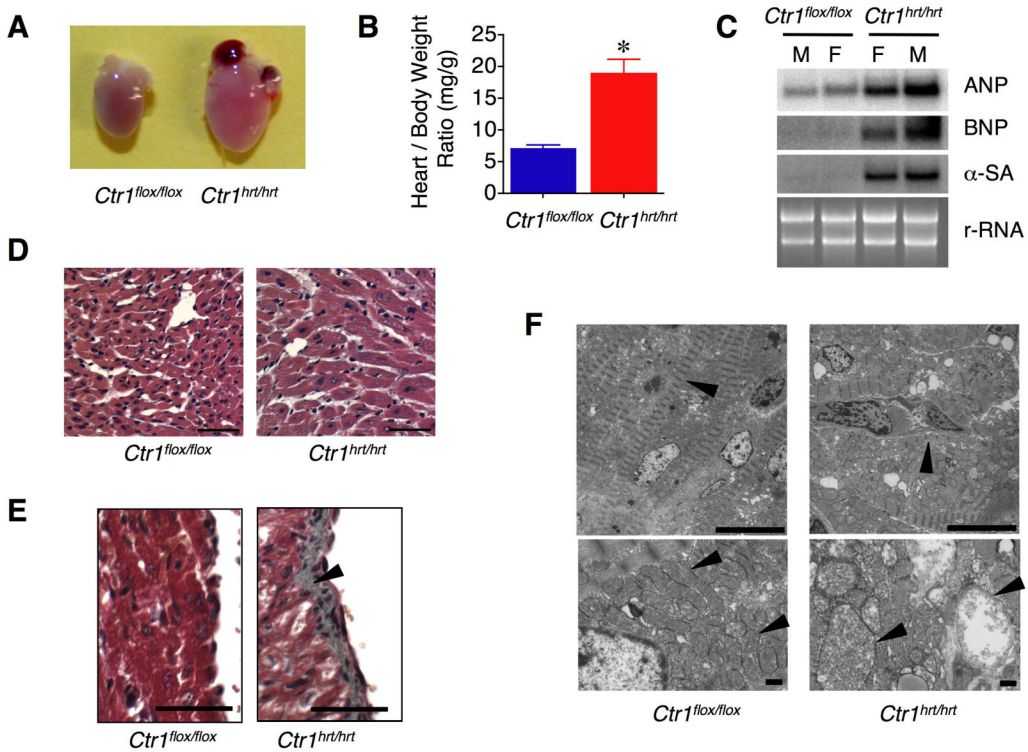

Figure 3. *Ctr1*$^{hrt/hrt}$ mice exhibit cardiac hypertrophy

(**A**) Gross morphology of P10 hearts from *Ctr1*$^{flox/flox}$ and *Ctr1*$^{hrt/hrt}$ mice. (**B**) Quantitation of heart weight/body weight ratio from *Ctr1*$^{flox/flox}$ (blue, n=7) and *Ctr1*$^{hrt/hrt}$ (red, n=7) mice. Error bars, s.d., $P < 0.0001$ versus *Ctr1*$^{flox/flox}$. (**C**) Markers of cardiac hypertrophy. Heart-specific mRNA from male and female *Ctr1*$^{flox/flox}$ and *Ctr1*$^{hrt/hrt}$ mice was analyzed by RNA blotting using ^{32}P-labeled DNA probes to atrial natriuretic peptide (ANP), b-type natriuretic peptide (BNP) and skeletal actin (SA). Ribosomal RNA (rRNA) is shown as a loading control. (**D**) Heart sections from P10 *Ctr1*$^{flox/flox}$ and *Ctr1*$^{hrt/hrt}$ were stained with hematoxylin and eosin. Left panel: *Ctr1*$^{flox/flox}$; right panel: *Ctr1*$^{hrt/hrt}$ (40X magnification; Scale Bar=50 μm). (**E**) Representative cardiac sections stained with Masson Trichome demonstrates extensive fibrosis (gray staining) in the ventricular endocardium region of tissue from *Ctr1*$^{hrt/hrt}$ mice, indicated with an arrowhead, as compared to *Ctr1*$^{flox/flox}$ controls (40X magnification; Scale Bar=50 μm). (**F**) Electron microscopy of cardiac tissue (1800X magnification of cardiac thin sections; upper panels, 3000X magnification of cardiac thin sections; lower panels, Scale Bar=1μm). Left panels, *Ctr1*$^{flox/flox}$; right panels, *Ctr1*$^{hrt/hrt}$. Thin section electron micrographs of cardiac tissues from *Ctr1*$^{hrt/hrt}$ mice show abnormally enlarged mitochondria with disrupted cristae structures. Myofilaments and mitochondria are indicated with arrowheads.

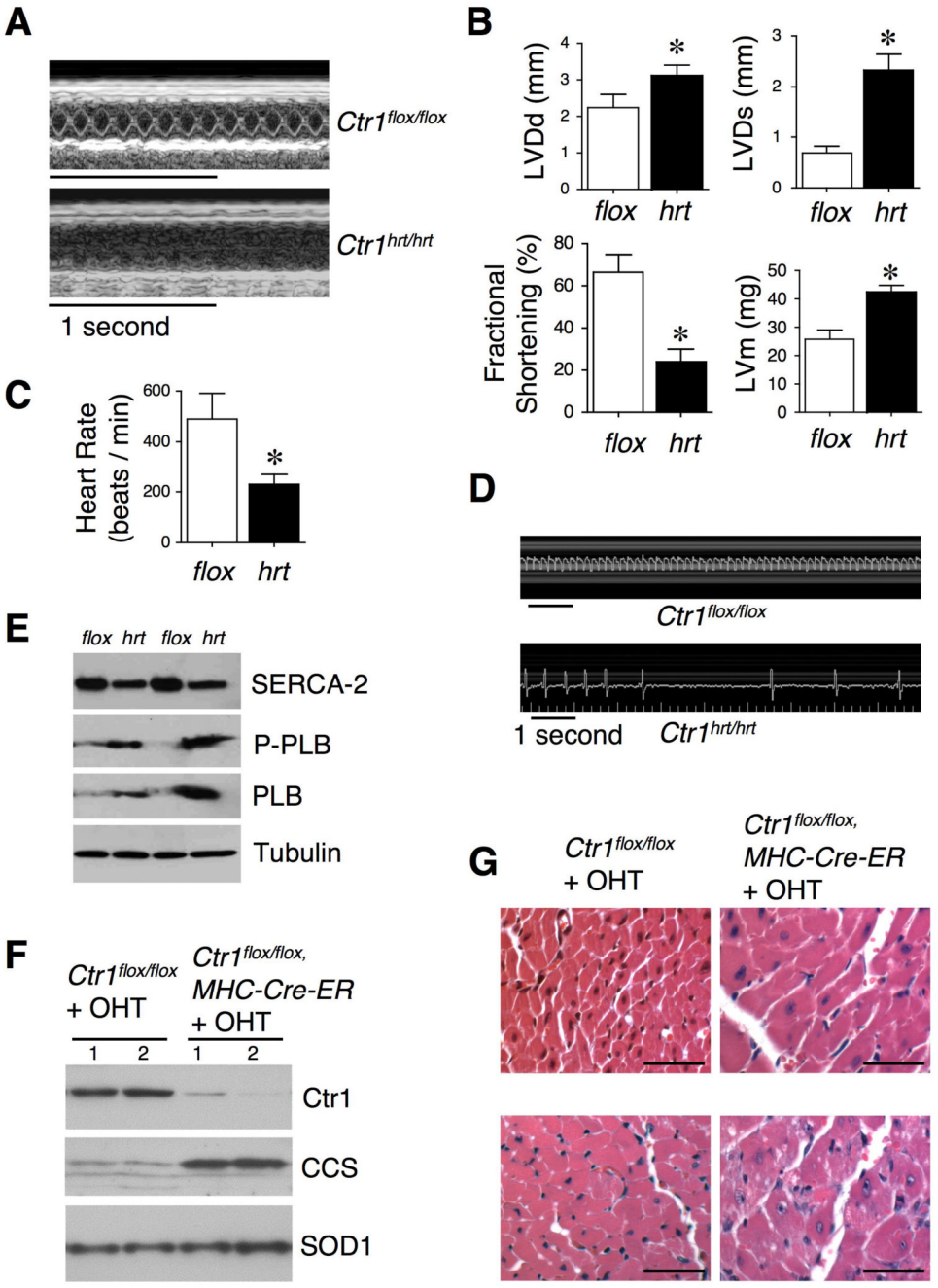

Figure 4. Cardiac dysfunction resulting from loss of the Ctr1 Cu ion channel

(**A**) Representative echocardiogram M-mode images from *Ctr1*$^{flox/flox}$ and *Ctr1*$^{hrt/hrt}$ at postnatal 10 days. (**B**) Quantitation of left ventricular diastolic dimension (LVDd), left ventricular systolic dimension (LVDs), fractional shortening and left ventricular mass (LVm) for *Ctr1*$^{flox/flox}$ (n=10) and *Ctr1*$^{hrt/hrt}$ mice (n=9). Error bars, s.d. *P < 0.0001 versus *Ctr1*$^{flox/flox}$. (**C**) Mouse heart rate measurements demonstrate a ~ 50% decrease in heart rate in *Ctr1*$^{hrt/hrt}$ mice (n=10) relative to control mice (n=9). Error bars, s.d., *P < 0.0001 versus *Ctr1*$^{flox/flox}$. (**D**) Electrocardiographic analysis of *Ctr1*$^{flox/flox}$ and *Ctr1*$^{hrt/hrt}$ mice from P10 reveal a bradycardia due to cardiac-specific loss of Ctr1. (**E**) SDS-PAGE analysis of total heart extracts of two independent *Ctr1*$^{flox/flox}$ (*flox*) and two independent *Ctr1*$^{hrt/hrt}$ mice (*hrt*).

Immunoblots were probed for SERCA-2, P-PLB (phospho-phospholamban, Ser-16), PLB (phospholamban) and Tubulin as a loading control. (**F**) Immunoblot of cardiac tissues for Ctr1, CCS and SOD1 (included as loading control) from two representative 2 month-old *Ctr1*$^{flox/flox}$ mice and two *Ctr1*$^{flox/flox}$*; MHC-Cre-ER* mice after tamoxifen (OHT) treatments. 1 and 2 indicate samples from two independent mice of each genotype. (**G**) Heart sections from 2 month and 7 month-old *Ctr1*$^{flox/flox}$ and *Ctr1*$^{flox/flox}$*; MHC-Cre-ER* mice injected with OHT were stained with hematoxylin and eosin. Left panel: *Ctr1*$^{flox/flox}$, right panel: *Ctr1*$^{flox/flox}$*; MHC-Cre-ER* (40X magnification, Scale Bar=50 μm).

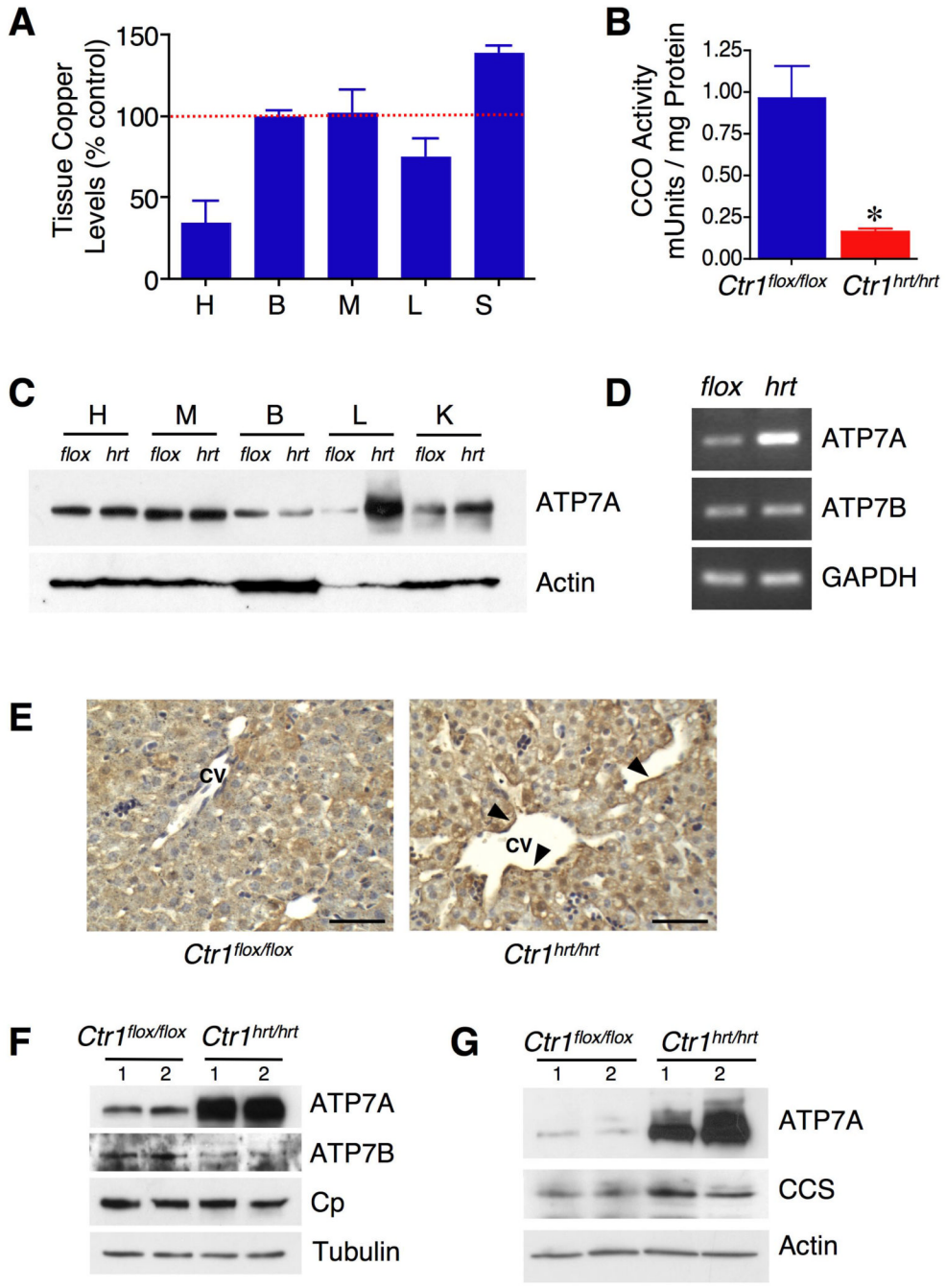

Figure 5. ATP7A expression is increased in the liver and intestine of *Ctr1*$^{hrt/hrt}$ mice

(**A**) Tissue Cu levels in *Ctr1*$^{hrt/hrt}$ mice are shown as a percentage of Cu levels from *Ctr1*$^{flox/flox}$ mice (100%). Error bars, s.d., *P < 0.005 versus Cu levels in *Ctr1*$^{flox/flox}$. H, heart; B, brain; M, muscle; L, liver; S, serum. (**B**) Mitochondrial cytochrome oxidase activity in cardiac tissue from *Ctr1*$^{flox/flox}$ (blue, n=4) and *Ctr1*$^{hrt/hrt}$ (red, n=5) mice. Error bars, s.d., *P < 0.005 versus *Ctr1*$^{flox/flox}$. (**C**) Immunoblot of representative *Ctr1*$^{flox/flox}$ *(flox)* and *Ctr1*$^{hrt/hrt}$ *(hrt)* mouse tissues for ATP7A and Actin (as loading control). H, heart; M, muscle; B, brain; L, liver; K, kidney. (**D**) Semi-quantitative RT-PCR for ATP7A and ATP7B. GAPDH was assayed as an input control. (**E**) Immunohistochemistry of *Ctr1*$^{flox/flox}$ and *Ctr1*$^{hrt/hrt}$ mouse liver with anti-ATP7A antibody. Enriched ATP7A expression toward the sinusoidal

space is indicated with arrowheads. The central vein (CV) is indicated. Scale Bar=50μm. (**F**) Immunoblot analysis of total Triton X-100 solubilized liver extracts from two representative *Ctr1*$^{flox/flox}$ and *Ctr1*$^{hrt/hrt}$ mouse tissues for ATP7A, ATP7B and ceruloplasmin (Cp) and Tubulin as a loading control). (**G**) Immunoblot analysis of ATP7A and CCS in the intestinal epithelial cells of two representative *Ctr1*$^{flox/flox}$ and *Ctr1*$^{hrt/hrt}$ mice. Actin levels were assayed as a loading control. For panels F and G, 1 and 2 indicate samples from two independent mice of each genotype.

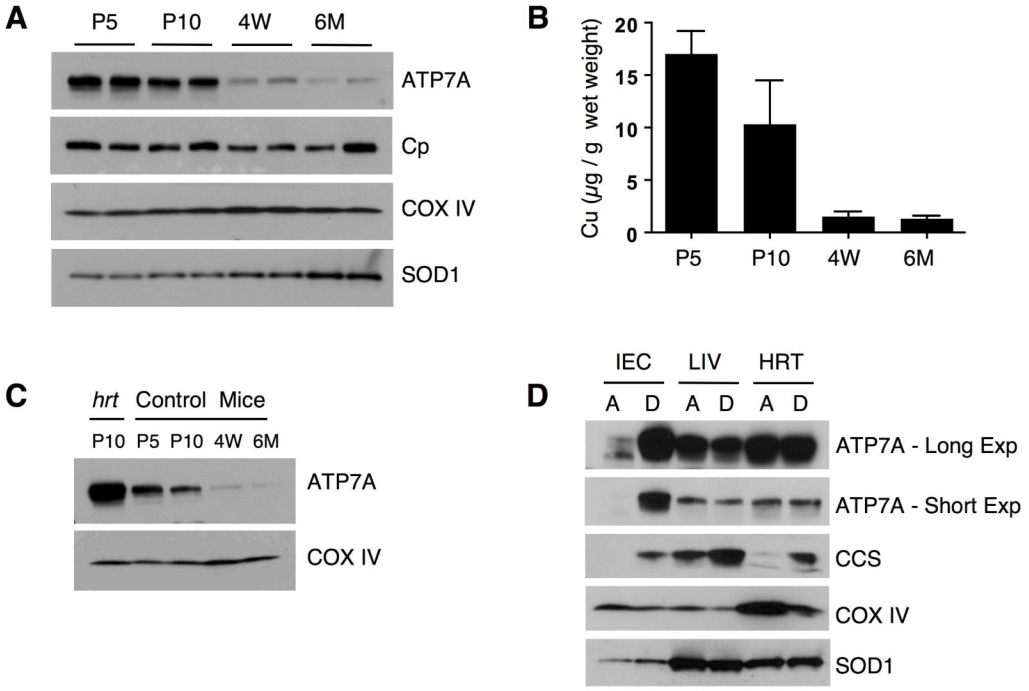

Figure 6. ATP7A expression correlates with hepatic Cu mobilization

(**A**) Immunoblot analysis of ATP7A, Ceruloplasmin (Cp), COX IV and SOD1 in the liver of wild type C57BL mice during maturation. P5; postnatal day 5, P10; postnatal day 10, 4W; 4 week-old mice, 6M; 6 month-old mice. (**B**) Liver Cu levels from wild type mice. P5; postnatal day 5, P10; postnatal day 10, 4W; 4 week-old mice, 6M; 6 month-old mice. Error bars, s.d., n=5 for each group. (**C**) Comparison of hepatic ATP7A levels between a representative 10 day old *Ctr1*$^{hrt/hrt}$ (*hrt*) mouse and wild type mice at P5; postnatal day 5, P10; postnatal day 10, 4W; 4 week-old mice, 6M; 6 month-old mice. (**D**) ATP7A expression levels (short exposure as well as longer exposure shown) in the intestinal epithelial cells (IEC), liver (LIV) and heart (HRT) in response to a Cu-limited diet in wild type C57BL mice. CCS and COX IV were assayed as cellular Cu level indicators and SOD1 is shown as a loading control. A indicates a copper adequate diet and D indicates a copper deficient diet.

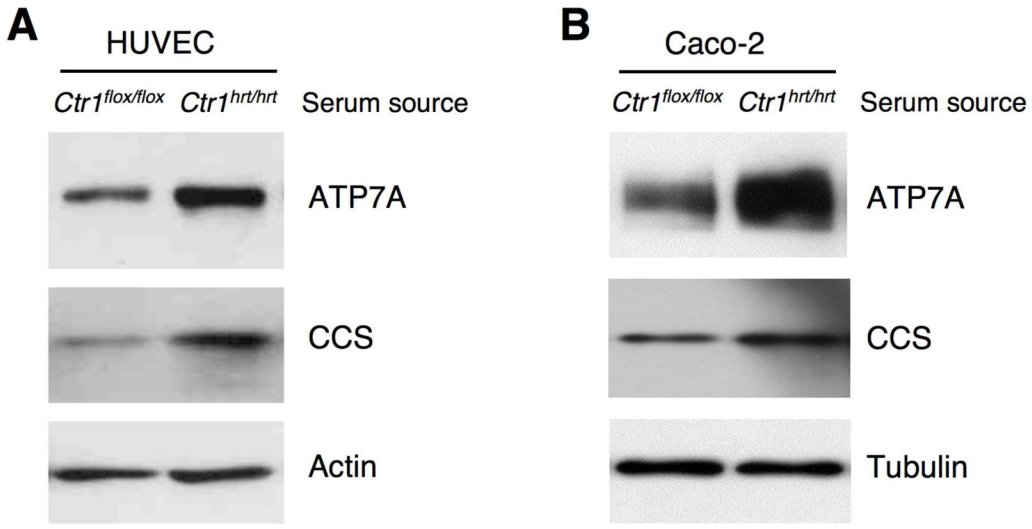

Figure 7. *in vitro* activation of ATP7A protein in serum treated human cells

(**A**) Immunoblot analysis of ATP7A and CCS levels in HUVEC cells treated with serum from control *Ctr1*$^{flox/flox}$ and *Ctr1*$^{hrt/hrt}$ mice. Actin levels were assayed as a loading control. (**B**) Immunoblot analysis of ATP7A and CCS levels in Caco-2 cells treated with serum from control *Ctr1*$^{flox/flox}$ and *Ctr1*$^{hrt/hrt}$ mice. Tubulin levels were assayed as a loading control. The source of the serum is indicated by the mouse genotype.